Smart Radio Environment via a Network of Distributed Tags acting as a Reconfigurable Intelligent Surface

Journal:	*IEEE Journal of Radio Frequency Identification*
Manuscript ID	JRFID-0078-04-2025
Manuscript Type:	Special Section: Selected Papers from the 2025 IEEE International Conference on RFID Technology and Applications
Date Submitted by the Author:	28-Apr-2025
Complete List of Authors:	Michalak, Lilian; Institut National des Sciences Appliquees de Lyon Centre des Humanites Assogba, Ognadon; Universite Claude Bernard Lyon 1 Sanchez, Daniel Raposo; Institut National des Sciences Appliquees de Lyon Centre des Humanites Villemaud, Guillaume; Institut National des Sciences Appliquees de Lyon Centre des Humanites Duroc, Yvan; Universite Claude Bernard Lyon 1
Keywords:	chipless RFID < RFID, energy and power transfer < RFID, modeling and simulation < RFID, RFID applications < RFID, RFID tag < RFID

Smart Radio Environment via a Network of Distributed Tags acting as a Reconfigurable Intelligent Surface

Lilian Michalak, Ognadon Assogba, Daniel Raposo Sanchez, Guillaume Villemaud, *Senior Member, IEEE,* Yvan Duroc, *Senior Member, IEEE*

***Abstract*— This paper aims to demonstrate that a network of tags can be 'controlled' (or configured) to improve communication between two radio nodes, using the same principle as for reconfigurable intelligent surfaces (RIS). RIS enables dynamic, targeted control of radio signals between a transmitter and a receiver, considering the propagation environment to optimize the radio link. However, RIS have to be specially deployed, and face the problem of remote control and energy supply. Assuming that future generations of passive RFID tags will incorporate the ability to switch between different load impedances in a reader-controlled way, the concept proposed here is to use tag networks already present in the environment as RIS. In addition to demonstrating this concept through several scenarios, the aim here is to introduce and compare different strategies for optimizing the choice of load impedances. The proposed analysis is also based on two modeling approaches: the first, based on the Friis equation, provides a clear illustration of the concept and its issues; the second, more general and realistic, is based on an *N*-port electrical equivalent model, and enables us to consider tag networks with more complex geometries, with no constraints on inter-tag distances. The results obtained are promising and demonstrate the potential of such an approach.**

***Index Terms*—Radio Frequency Identification, Reconfigurable Intelligent Surface, Wireless Power Transfer**

I. INTRODUCTION

THE constant pursuit to improve the efficiency and reliability of wireless communication networks has led to the exploration of new methods and materials for propagating electromagnetic signals. In recent years, Reconfigurable Intelligent Surfaces (RIS), equipped with a large number of passive reflective elements connected to a programmable intelligent controller, have emerged as an emerging technology capable of completely transforming wireless communication networks [1]. Thanks to their ability to dynamically and intelligently manipulate electromagnetic waves in their propagation environment, RIS can significantly improve signal quality, spectral and energy efficiency, and extend coverage in wireless networks [2, 3].

Recently, significant progress has been made in several areas with the introduction of RIS technology [4]. Despite a wide range of potential applications in wireless communications [5] and the benefits they offer [6, 7], RIS technology faces numerous obstacles. One issue is the high cost of RIS surfaces, as they require many individually controllable cells, the maintenance and upkeep of which can be expensive [8]. RIS also involve complex and power-hungry control algorithms to enable each element to adapt to changing propagation channel conditions [9].

Radio Frequency Identification (RFID) technology is a potential alternative because of its low cost, low power consumption and the wireless connectivity it can offer [10]. Feasibility studies have shown that a network of RFID tags can be used to control the behavior of a RIS by wirelessly programming a tag's microchip [11, 12]. To solve the problems of power consumption and complexity associated with RIS, a network of almost passive RFID tags powered by a programmable reader to optimize the gain of the RIS surface, with a classical regular grid pattern, is proposed in [13]. RFID tags, widely used for tracking and identification purposes, could therefore be repurposed as passive elements in a RIS, contributing to signal manipulation without the need for additional power sources, thus offering a cost-effective and scalable approach to RIS deployment.

The aim of this work is, firstly, to demonstrate the potential of a reconfigurable distributed RFID tag network by dynamically adjusting the load impedances of so-called reflector tags to induce constructive interference towards a target tag queried by a distant RFID reader (or indeed any other source). The idea developed in this article is that by adapting the operation of an already existing RFID tag network to that of a RIS, it would be possible to create intelligent environments that could improve the performance of wireless communication efficiently and cost-effectively by taking advantage of the

Manuscript submitted April 28, 2025.

L. Michalak was with the CITI laboratory, Lyon University, INSA Lyon, INRIA, Villeurbanne, F-69100, France (e-mail: lilian.michalak@insa-lyon.fr).

O. Assogba is with the University Claude Bernard Lyon 1, Ampere, UMR5005, INSA Lyon, Ecole Centrale de Lyon, CNRS, Villeurbanne, F-69100, France (e-mail: ognadon.assogba@univ-lyon1.fr).

D.R. Sanchez was with the CITI laboratory, Lyon University, INSA Lyon, INRIA, Villeurbanne, F-69100, France (e-mail: d.raposo@alumnos.upm.es).

G. Villemaud is with the CITI laboratory, Lyon University, INSA Lyon, INRIA, Villeurbanne, F-69100, France (e-mail: guillaume.villemaud@insa-lyon.fr).

Y. Duroc is with the University Claude Bernard Lyon 1, Ampere, UMR5005, INSA Lyon, Ecole Centrale de Lyon, CNRS, Villeurbanne, F-69100, France (e-mail: yvan.duroc@univ-lyon1.fr).

existing capabilities of RFID. For instance, in a large warehouse scenario, where a high density of RFID tags is already present, it appears to be interesting to benefit from the potential reshaping of the radio channel via the choice of the optimal loads of all or a subset of these tags to enhance the radio link between two particular points in the space of this warehouse. In such a scenario, RFID-based distributed RIS could enhance coverage and signal quality in complex areas with dense structures, ensuring extended range for RFID applications or even reliable connectivity for other IoT devices and other wireless applications. By addressing challenges such as signal propagation and coverage in a cost-effective and energy-efficient manner, RFID-based distributed RIS could play a crucial role in the development of next-generation wireless networks, deployed in environment containing tagged objects.

The outline of this paper is as follows. Section II presents the proposed idea, based on a simplified modeling approach that provides a clear initial conceptual analysis. Several strategies for selecting the load impedances of reflector tags are also introduced and analyzed. The proposed examples consider a relatively dense tag network, with 30 tags for the illustration. Section III introduces a second model, more realistic and general than the previous one, and moreover, more efficient in terms of complexity and computation time than other possible approaches. Starting from a network with only 2 or 4 tags (but without loss of generality), the examples proposed complete the previous analysis, particularly for the strategy based on a differential evolution algorithm. Conclusions and perspectives are drawn in Section IV.

II. Presentation of The Concept In The Context Of Approximating The Friis Equation

A. Modeling Principle and Associated Assumptions

Let us consider a network of UHF (Ultra High Frequency) RFID tags (sufficiently distant from each other to be considered in the far field relative to each other) and placed in the far field relative to a reader.

Assuming the reader is in continuous wave mode, the aim is to determine the power received by one of the tags in the network, called the target tag and denoted Tag_0, considering both the direct path (the one in direct view) and the indirect paths (reflected by the other tags towards the target tag).

Considering that the propagation environment contains only the system described (i.e., there are no other objects present), that all the tags are of the same type, have the same antenna which is of the dipole type, are placed in the same plane perpendicular to it, and likewise for the reader, then [14] showed that the power received by the target tag, P_{Tag_0}, is written as follows:

$$P_{Tag_0} = P_t G_t G_{T_0} \left(\frac{\lambda}{4\pi R_0}\right)^2 \left[1 + \sum_i \sqrt{\frac{\sigma_i}{4\pi}} \frac{R_0}{R_i d_i} exp\left(j\theta_{d_i}\right)\right]^2 \quad (1)$$

with P_t and G_t the emitted power and the antenna gain of the RFID reader respectively, G_{T_0} the antenna gain of the target tag, λ the wavelength, R_0 and R_i the distances from RFID reader to Tag_0 and each i^{th} reflector tag (Tag_i) respectively, d_i the distance between Tag_0 and each Tag_i.

θ_{di} is the relative phase difference of the direct signal from the RFID reader and the indirect signal from each Tag_i arriving on Tag_0 and is defined as follows:

$$\theta_{di} = \frac{2\pi}{\lambda}[(R_i + d_i) - R_0] \quad (2)$$

σ_i is the bistatic radar cross section (RCS) and is defined as follows:

$$\sigma_i = \frac{G_{T_i}^2 \lambda^2}{4\pi} K_i \quad (3)$$

where for each i^{th} reflector tag, G_{T_i} is the antenna gain, $K_i = |1 - \Gamma_i^*|^2$ is the ratio of the power of the backscattered signal to the power of the incident signal with Γ_i^* the power reflection coefficient such as:

$$\Gamma_i^* = \frac{Z_{L_i} - Z_A^*}{Z_{L_i} + Z_A^*} \quad (4)$$

with Z_A and Z_L are the complex antenna and load impedances respectively.

Note the following special cases: $K = 1$, when antenna and load impedances are matched (i.e., $Z_L = Z_A^*$), the tag is in receive mode, energy recovery is favored, limiting reflection; $K = 4R_A^2/(R_A^2 + X_A^2)$ with R_A and X_A the resistive and reactive parts of Z_A respectively, when the antenna is short-circuited (i.e., $Z_L = 0$); $K = 0$, when the antenna is open-circuited (i.e., infinite load impedance), the tag is in an ideal absorption mode (the tag does not reflect any waves); $K = 4$, when the load impedance is equal to the conjugate of the imaginary part of the antenna impedance (i.e., $Z_L = -jX_a$), the tag is in maximum reflector mode.

As a result, the power received by the target tag is not only dependent on the power transmitted by the reader, but is also highly dependent on the position of each of the reflector tags (the reflected wave adds constructively or destructively to the direct path) and on the impedance of the load connected to them (the intensity of the reflected wave is greater or less). Consequently, each reflector tag acts favorably or unfavorably on the total amount of power received by the target tag.

B. Binary Consideration of the Constructiveness

To illustrate the proposed concept, a network of 30 tags is considered, consisting of a target tag around which 29 reflector tags have been randomly distributed within a radius of 7.5λ. The source with coordinates $(0, -60\lambda)$ is located at a distance of 60λ and the emitted power is 30 dBm. The number of tags and the different distances have been chosen arbitrarily, without loss of generality as to the principle. For this example, the so-called *Binary* strategy is considered: each reflector tag is either in total reflector mode ($K = 4$) or in total absorption mode ($K = 0$).

As illustrated by Fig. 1, with the aim of maximizing the power received by the target tag, the loading of each reflector is chosen according to whether the resulting reflected wave is

destructive or constructive. Note that the impact on the power received by the target tag will be quantified in the study in the following subsection.

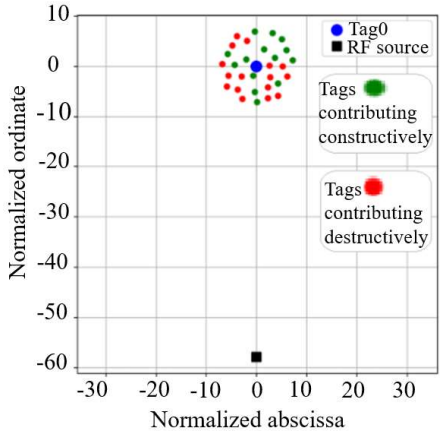

Fig. 1. Binary strategy configuration with 29 reflector tags and a target tag in far field with respect to a reader.

C. Extended Strategies to Set Load Impedances

With the aim of quantifying the power received by the target tag and the impact of the reflector tag network, the previous study is extended by considering several strategies. To the previous *Binary* strategy, the following cases are added: the *NoReflect* case for which only the target tag is present, which will serve as a reference; the *AllReflect* strategy for which all 29 reflector tags have their antennas short-circuited; and the *DE* strategy for which a Differential Evolution (DE) algorithm is introduced which aims to optimize the power received by the target tag by calculating the most favorable continuous set of reflector load impedances.

The use of evolutionary metaheuristics (like DE) to optimize load impedances in a reconfigurable RFID network is fully justified by the non-convex nature of this problem and its dimensions [15]. This choice is based on:

- a black-box objective function (received power) evaluated by electromagnetic (EM) calculation;
- an algorithm that is robust to local minima, capable of handling a large number of variables and a potentially very large search space;
- a compromise between computation time and accuracy: if necessary, the choice of impedances is limited to a few discrete values (see section III);
- the use of the python library ('*scipy.optimize*') to facilitate the automation of simulation and direct integration with EM modeling (see also section III).

A Monte Carlo simulation (50 repetitions) is carried out for the three cases with the presented tag network, based on the following principle: i) the configuration of the tag network is randomly drawn (same hypothesis as in the previous section, i.e., random position of the 29 reflector tags around the target tag within a radius of 7.5); ii) depending on the strategy, the load impedances of each reflector tag are determined; iii) the total power received by the target tag is calculated. Without loss of generality, for simulation purposes the power transmitted by the reader is set arbitrarily (also in line with regulations) at 30 dBm.

Fig. 2 shows the results obtained for the four strategies considered: the value of the power received is on the x-axis, and the number of occurrences corresponding to this value on the y-axis. In the case where there are no tags in the vicinity of the target tag, the latter receives power from the reader equal to -23.2 dBm. In the case of the *AllReflect* strategy, the power received varies between about -24 dBm and -21 dBm, which shows that, depending on the relative position of the tags, the reconstruction of the paths reflected at the target tag can be constructive or destructive. The *Binary* strategy illustrates the advantage of considering only those tags that make a positive contribution (linked to their position); the gain here is at least -22.5 dBm up to -20 dBm. Finally, the *DE* strategy improves performance, but its parameters do not lead to better results than the *Binary* strategy.

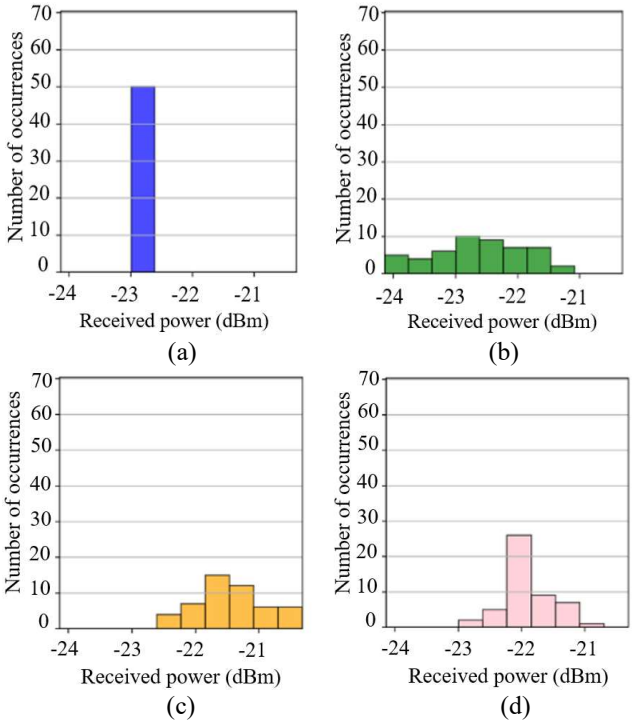

Fig. 2. Histogram illustrating the received power by the target tag: a) *NoReflect* case; b) *AllReflect* strategy; c) *Binary* strategy; d) *DE* strategy.

III. Generalization Of The Model And Application Examples

Modeling using the Friis equation is constrained by far-field propagation conditions, considers electrical quantities only in terms of power (and therefore does not consider phase terms), and does not consider mutual coupling between radiating elements. These constraints are very limiting, and mean that only simplified or even reduced geometric configurations can be envisaged. On the other hand, the use of an EM simulator

such as CST Microwave Studio or HFSS, for instance, entails very high calculation costs (and therefore also long calculation times, depending on the computer). This is especially true as the electromagnetic simulation must be repeated for each change in the set of load impedances.

A. Modeling the Tag Network using an N-port Equivalent Circuit Model

To overcome these limitations, one possibility is to model the tag network using an equivalent circuit model, which provides access to currents and voltages, as well as considering electromagnetic aspects. From [16], the tag network can be modeled as an N-port electrical circuit, as shown in Fig. 3. Each antenna is modeled as a Thevenin generator linked to an impedance matrix, which allows the various mutual couplings to be considered.

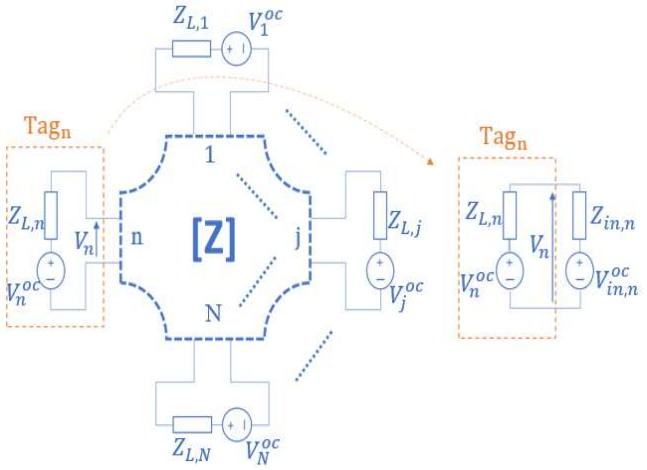

(a) (b)

Fig. 3. Equivalent circuit model of: (a) N loaded tag antennas exposed to a n incident electromagnetic wave; (b) the equivalent circuit seen by the nth tag antenna (reformatted from [16]).

In this electrical model, the input impedance seen by the nth port ($Z_{in,n}$) represents the effective impedance that tag n "sees" when considering its own load, mutual coupling, and the loads of the other tags. This impedance determines how the open-circuit voltage is distributed between the antenna ($V_{in,n}^{oc}$) and the load of the tag (V_n^{oc}), and enables to calculate the amount of power ultimately absorbed or reflected by the nth port.

To calculate $Z_{in,n}$ a local modification of the classic impedance matrix $\boldsymbol{Z}$ is performed by adding the loads $\{Z_{L,j}\}$ to the corresponding diagonals of $\boldsymbol{Z}$ (except for the nth column, according to the established convention). Note that $\boldsymbol{Z}$ considers the self-impedances of each antenna (diagonal terms) and the mutual impedances, which are a function of the geometry and orientation of the antennas, the distance between them and the frequency. The new relation of the modified impedance matrix $\boldsymbol{Z_{modn}}$ presents the impedance $(Z_{jj} + Z_{L,j})$ at each diagonal and allows for the consideration of the load impedance of each tag.

$$\boldsymbol{Z_{modn}} = \begin{pmatrix} Z_{11}+Z_{L,1} & \cdots & Z_{1n} & \cdots & Z_{1N} \\ \vdots & \ddots & \vdots & & \vdots \\ Z_{j1} & \cdots & Z_{jj}+Z_{L,j} & \cdots & Z_{jN} \\ \vdots & & \vdots & \ddots & \vdots \\ Z_{n1} & \cdots & Z_{ni} & Z_{nn} & Z_{nN} \\ \vdots & & \vdots & & \vdots \\ Z_{N1} & \cdots & Z_{Ni} & \cdots & Z_{NN}+Z_{L,N} \end{pmatrix} \quad (5)$$

From (5), the input impedance, $Z_{in,n}$, which takes into account both mutual impedances and the impedances of load on other ports ($Z_{L,n}$), is deduced as follows:

$$Z_{in,n} = \frac{1}{[\boldsymbol{Z_{modn}^{-1}}](n,n)} \quad (6)$$

and this gives the power reflection coefficient, $\Gamma_{int,n}$, such as:

$$\Gamma_{int,n} = \frac{Z_{Ln} - Z_{in,n}^*}{Z_{Ln} + Z_{in,n}}. \quad (7)$$

A good impedance matching (i.e., low value of $|\Gamma_{int,n}|$) indicates efficient power transfer to the tag. Thus, by modifying the load impedance of the antenna ($Z_{L,n}$), $\Gamma_{int,n}$ is affected and, consequently, the absorbed or re-emitted power. For a nearly matched load ($Z_{L,i} \approx Z_A^*$), $|\Gamma_{int,i}| \approx 0$, which minimizes backscattering and maximizes absorption. On the other hand, a purely reactive load ($Z_{L,i} = jX_A$) can maximize reflection ($|\Gamma_{int,i}| = 1$) and adjust the phase of the reflected signal. The combined effect of the loads $\{Z_{L,i}\}$ influences the phases and amplitudes of the reflected signals. One can optimize each Z_L so that the signals add constructively at the target tag location. This requires managing multiple mutual interactions and carefully adjusting the $\Gamma_{int,i}$.

Thanks to this modeling, open-circuit voltages (V^{oc}), load impedances (Z_L) and the $\boldsymbol{Z}$ impedance matrix are the main input parameters for the simulation. In this work, PyNEC has been used to calculate this $\boldsymbol{Z}$ matrix. PyNEC is a Python library that allows simulating and analyzing antenna structures and their electromagnetic behavior using the Node and Element Method (Numerical Electromagnetics Code, NEC) developed to solve 3D electromagnetism problems, particularly for single antenna and antenna array analysis. PyNEC is primarily designed for simple structures, particularly wire antennas and wire antenna arrays with geometries that can be processed using the NEC method. After comparisons, this software offers the best tradeoff between complexity, calculation time and accuracy, enabling to model any configuration of tag networks (no restrictions to a single plane, no assumptions on the polarization nor the direction of the source, capturing nearfield and farfield behavior).

The following steps are therefore significantly simplified: i) the currents (I_n) at the ports are obtained directly from the electromagnetic simulation (PyNEC); ii) the $\boldsymbol{Z}$ impedance matrix is determined or updated using dedicated algorithms, without the need to restart cumbersome 3D-simulations; iii) the secondary electrical quantities (V_n, $V_{in,n}^{oc}$, etc.) are easily calculated from these data, thanks to the fundamental relationships derived from the N-port equivalent circuit model.

When a load impedance $Z_{L,j}$ is modified, it is not just the input

impedance of j[th] port that is changed, but all the input impedances of other ports. Consequently, a given complex load impedance value chosen for the reflector can have a positive or negative effect on the target tag, depending on the geometry and phase of the signals. Based on this formulation, the DE algorithm described in section II.C. could be applied with the objective of maximizing the received power at the desired tag.

B. Application Examples

Considering that in a real multi-tag scenario the values of load impedances need to be optimized, and that this optimization problem could lead to high computational costs, in this subsection this problem is addressed in three steps. First, a simple case with just one reflector tag is considered, in order to analyze the required range of load impedances that is appropriate to ensure a close-to-optimal gain at the receiver tag. Then, with the same topology, the question of the sufficient number of discrete values for the imaginary part of the load is investigated. Finally, using these aforementioned finite range and discrete values, a more complex scenario with multiple reflector tags is evaluated.

First case: 2-tag network

To first illustrate the impact of load optimization by using the N-port circuit model, previous configuration used for illustration purposes (see Section II) is repeated, but reduced to a single reflector tag whose distance from the target tag is varied (Fig. 4). The distance R_0 between the target tag and the reader is maintained at 60λ, and the transmitted power is also constant (30 dBm).

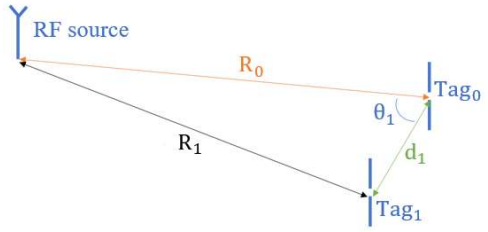

Fig. 4. Illustration of the studied scenario (inspired from [16]): Tag_0 (the target tag) and Tag_1 (the reflector tag) are separated by a distance d_1 and are distant from the RF source by distances R_0 and R_1 respectively.

To further investigate the actual limitations of implementing this approach, an additional strategy is introduced: *DEdiscrete* where the DE algorithm is applied for only discrete values over a limited range. Fig. 5 shows the received power at the target tag that is evaluated depending on the distance (normalized with respect to the wavelength) between the two tags (Tag_0 and Tag_1). Compared to the baseline *NoReflect*, all other scenarios could offer higher values of received power. Nevertheless, the *AllReflect* one greatly depends on the distance, and destructive contributions occur. In the *DE* case, the comparison between Fig. 5a and Fig. 5b clearly shows that with a too limited range the performance is degraded. Choosing an appropriate range is therefore crucial to ensure that for any distance the contribution of the reflector is beneficial. This study has shown that a [−400 j, +400 j] range is sufficient to ensure reliable results. More generally, it could also be observed that for nearfield conditions, the impact of optimization is really important, and as the distance increases, the contribution to the received power will decay.

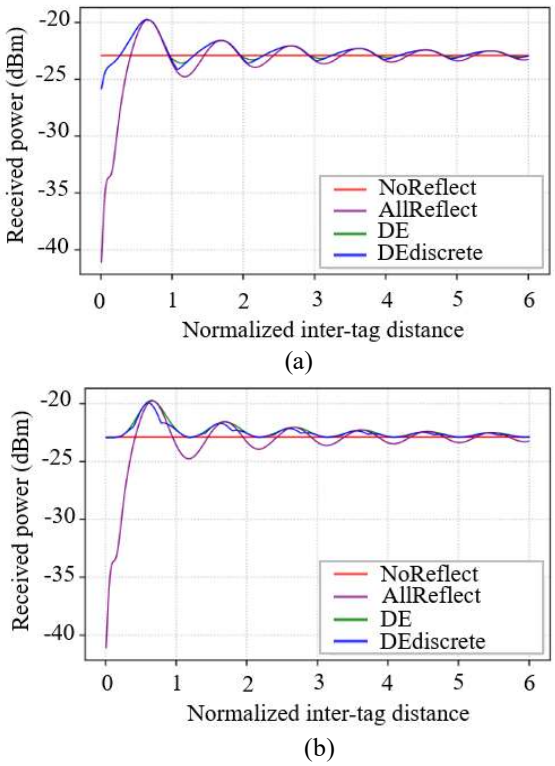

Fig. 5. Power received by the target tag as a function of the distance between the two tags, normalized to wavelength. The following cases are envisaged: *NoReflect* case; *AllReflect* strategy; *DE* strategy; *DEdiscrete* strategy such that the range of the imaginary part of the load impedance is: (a) [−50 j, +50 j] Ω ; (b) [−400 j, +400 j] Ω.

Second case: 2-Tag network with limited possible loads

As the algorithmic complexity of the *DE* strategy is penalizing, the aim here is to illustrate the impact of the finite number of load impedances considered in the exploration interval (here [−400 j, +400 j] Ω). Fig. 6 shows the same results than Fig. 5 but focusing on the *DE* strategy operated in discrete mode, i.e., the number M of possible load impedances in the interval under consideration is limited and such that $M = 3, 4, 5, 8$ or 11.

Odd values of M allow symmetrical values (positive and negative) in the range of reactance values considered, as well as the zero value; even values of M are also symmetrical, but the zero value is not considered. As expected, the results show that overall performance improves as M increases. However, the differences are not very significant, except for the case $M = 4$ (only 4 possible values, without the null value). The case $M = 5$ appears to be a good compromise between performance and complexity.

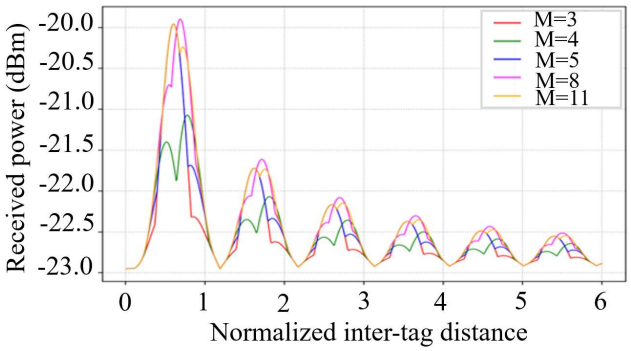

Fig. 6. Power on the receiver antenna for different numbers of states {M = 3, 4, 5, 8, 11} in the range of [−400 j, +400 j] Ω.

Third case: 4-tag network

The study is extended to the case of a network of 4 tags forming a square of side d as shown in Fig. 6. The distance R between the reader and the center of the network is here chosen equal to 150λ.

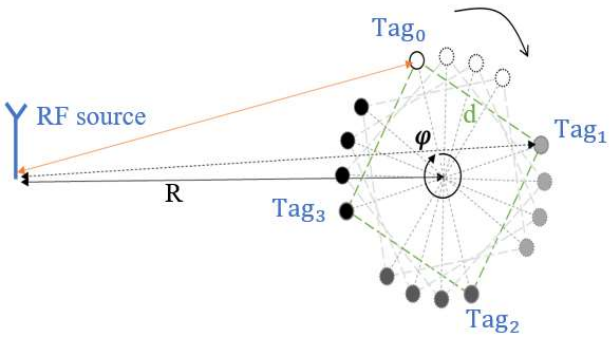

Fig. 7. Case of a 4-tag network forming a square located at distance R from the source. Tag_0 is chosen as the target tag, and the other Tags are used as reflectors.

Fig. 8 shows the power received by the target tag (Tag_0) as the tag array rotates, i.e., as the angle φ varies from 0 to 360 degrees. Two inter-tag distances are here presented: $d = 0.67\ \lambda$ (Fig. 8a) and $d = 2.5\ \lambda$ (Fig. 8b) for the different strategies. The results obtained highlight the importance of adjusting the load to control separately or jointly (depending on the implemented strategy) the amount of backscattered energy and the phase of the corresponding wave. In the *AllReflect* case, the received power by the target tag oscillates around the reference (*NoReflect* case, without reflector), depending on whether the reflected waves are constructive or destructive. To be able to obtain a gain in received power with this *AllReflect* strategy, the geometric configuration must be therefore controlled, which seems unrealistic with distributed tags outside a specific context, and this gain remains small compared with the other strategies that are presented.

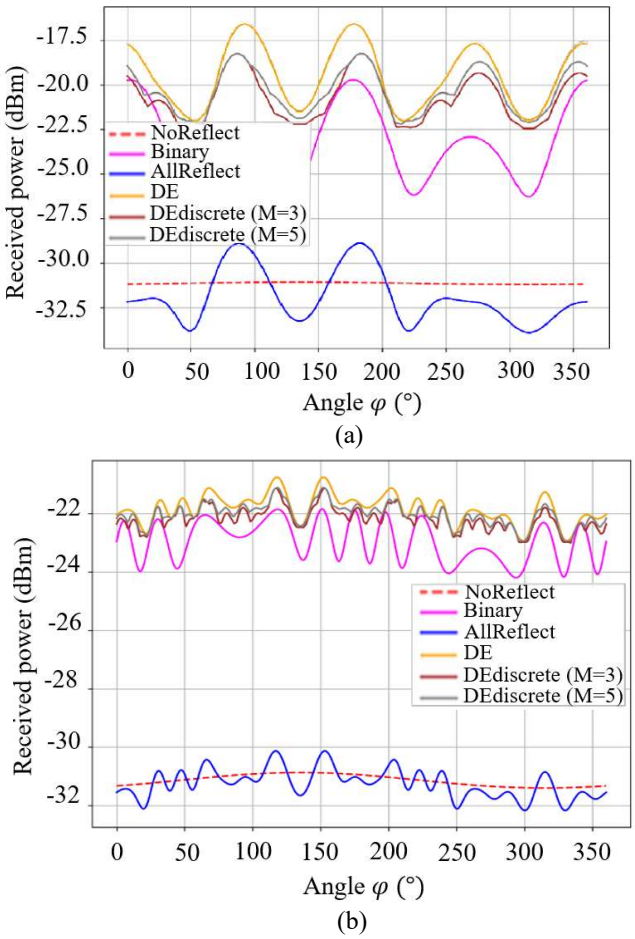

Fig. 8. Received power by Tag_0 as a function of φ, for: (a) $d = 0.67\ \lambda$, and (b) $d = 2.50\ \lambda$.

With the assumption of being able to set the appropriate load impedance of the reflector tags, the power received by the target tag is increased whatever the geometrical configuration. As expected, the gain is better with the *DE* strategy versus its discrete versions and the *Binary* strategy. Furthermore, as previously observed in Fig. 6, the *DE* algorithm used on only 5 states and a sufficient range achieves good results with reduced computational complexity. Finally, it should be noted that, as expected, the smaller the distance between tags, the greater the gain in power received by the target tag, with less attenuation of reflected paths. From this simple example, it can be observed that with a simple *Binary* strategy with 3 reflectors, the range of the system has been extended from 60λ to 150λ to obtain the same average received power of -23 dBm. Implementing several possible loads and an optimization algorithm could extend even further this range extension, with more stable results.

IV. Conclusion

This paper presented a new paradigm in which tags present in an environment are used as a network of reflector tags to optimize a radio link between two nodes, similar to the RIS principle.

To model such a scenario realistically, the Friis equation remains limited to special cases, and 3D EM simulators require (too) long computation times. Hence the proposal is there to use an N-port network-type model, which has the double advantage of being able to integrate all types of geometric configurations without requiring excessive complexity (in terms of computation).

The concept was demonstrated using several strategies for selecting load impedance values to optimize wireless energy transfer. The easiest strategy, i.e., placing all tags in reflector mode, is only valid for specific geometrical configurations where reflected waves add up. A more effective strategy, unconstrained by the geometrical configuration, is to "switch off" tags that reflect a destructive wave in relation to the direct path, and favor tags that reflect a constructive wave. This so-called *Binary* strategy can be further improved by using an optimization algorithm of the differential evolution type. At the cost of a higher number of load impedances, the DE algorithm offers more degrees of freedom and better optimization. However, the strategies analyzed and the scenarios considered show that the *Binary* strategy achieves a good compromise: simpler hardware implementation (only two loads to control), very fast computation time, and overall good performance.

However, this study has not considered any complex radio channel, and it can be forecast from our preliminary results that in a complex environment and with a large number of tags with uncontrolled orientations, allowing multiple discrete loads (like *DEdiscrete* case) will lead to higher performance in any configurations. To this end, a deeper study on the trade-off between the number of possible loads, the algorithmic complexity and the range extension has to be performed.

REFERENCES

[1] Y. Liu, X. Liu, X. Mu, T. Hou, J. Xu, M. Di Renzo and N. Al-Dhahir, "Reconfigurable intelligent surfaces: principles and opportunities," *IEEE Communications Surveys and Tutorials*, vol. 232021, no. 23, pp. 1546-1577, May 2021, doi : 10.1109/COMST.2021.3077737.

[2] L. Subrt, and P. Pechac, "Intelligent walls as autonomous parts of smart indoor environments," *IET Communications*, vol. 2, no. 6, pp. 1004-1010, May 2012, doi: 10.1049/iet-com.2010.0544.

[3] X. Yang, C.-K. Wen, and S. Jin, "MIMO detection for reconfigurable intelligent surface-assisted millimeter wave systems," *IEEE Journal on Selected Areas in Communications*, vol. 38, no. 8, pp. 1777-1792, Aug. 2020, doi: 10.1109/JSAC.2020.3000822.

[4] F. Naaz, A. Nauman, T. Khurshaid, and S.-W. Kim, "Empowering the vehicular network with RIS technology: a state-of-the-art review," *Sensors,* vol. 24, no. 2, pp. 337-372, Jan. 2024, doi:10.3390/s24020337.

[5] K. M. Faisaly, and W. Choi, "Machine learning approaches for reconfigurable intelligent surfaces: a survey," *IEEE Access*, vol. 10, no. 10, pp. 27343-27367, Jan. 2022, doi: 10.1109/ACCESS.2022.3157651.

[6] M. Min, J. Xiao, P. Zhang, J. Song, and S. Li, "Learning-based IRS-assisted secure transmission for mine IoTs," *Sensors,* vol. 23, no. 14, pp. 6321- 6337 July. 2023, doi:10.3390/s23146321.

[7] M.M. Silva, and J. Guerreiro, "On the 5G and beyond," *Applied Sciences.,* vol. 10, no. 20, pp. 7091-7103, Oct. 2020, doi: 10.3390/app10207091.

[8] S.M. Bukhari, H.M. Attaullah, S. Ali, and M.I. Aslam, 2023. "Wireless communications beyond antennas: the role of reconfigurable intelligent surfaces," in Proc. *International Conference on Emerging Trends in Electronic and Telecommunication Engineering*, Karachi, Pakistan, 2023, pp. 10-17.

[9] H.M. Attaullah, and I.A. Javed, "Wireless robotic car control through human interface using eye movement," *Interdisciplinary Journal of Applied and Basic Subjects*, vol. 1, no. 9, pp. 1-6, 2021.

[10] F. Costa, S. Genovesi, M. Borgese, A. Michel, F.A. Dicandia, and G. Manara, "A review of RFID sensors, the new frontier of internet of things," *Sensors,* vol. 21, no. 9, pp. 3138-3172, April 2021, doi:10.3390/s21093138.

[11] F. Lestini, G. Marrocco, and C. Occhiuzzi, "RFID-based reconfigurable intelligent surfaces: towards wireless and ultra-low-power reconfigurability," in Proc. *European Conference on Antennas and Propagation*, Glasgow, U.K., 2024, pp. 1-4.

[12] F. Lestini, G. Marrocco, and C. Occhiuzzi, "Feasibility of RFID-based control of reconfigurable intelligent surfaces (RISs) for wireless communication systems," in Proc. *IEEE International Conference on RFID Technology and Applications*, Aveiro, Portugal, 2023, pp. 241-244.

[13] I. Vardakis, G. Kotridis, S. Peppas, K. Skyvalakis, G. Vougioukas, and A. Bletsas, "Intelligently wireless batteryless RF-powered reconfigurable surface: theory, implementation and limitations," *IEEE Transactions on Wireless Communications*, vol. 22, no. 6, pp. 3942-3954, Jun. 2023, doi: 10.1109/TWC.2022.3222733.

[14] D. Ba, I. Diou, and Y. Duroc, "Theoretical considerations on the impact of nearby tags on the wireless power transfer from the reader to the target tag in Passive UHF RFID," *IEEE Journal of Radio Frequency Identification*, vol. 7, pp. 463-471, Aug. 2023, doi: 10.1109/JRFID.2023.3303962.

[15] A. Mughal, J.M. Sudersanan, S. Mostarshedi, B. Poussot, and J.M. Laheurte, "Statistical evaluation of the coupling effects between tags in a UHF RFID forward Link," *IEEE Journal of Radio Frequency Identification,* vol. 7, pp. 257-266, Jul. 2023, doi:10.1109/JRFID.2023.3293207.

[16] P.I. Lazaridis, E.N. Tziris, Z.D. Zaharis, T.D. Xenos, J.P. Cosmas, P.B. Gallion, V. Holmes, and I. A. Glover, "Comparison of evolutionary algorithms for LPDA antenna optimization," *Radio Science*, vol. 51, pp. 1377-1384, Aug. 2016, doi:10.1002/2015RS005913.